Differentiation of bacterial spores via 2D-IR spectroscopy

Barbara Procacci,[1] Samantha H. Rutherford,[2] Gregory M. Greetham,[3] Michael Towrie,[3] Anthony W. Parker,[3] Camilla V. Robinson,[4] Christopher R. Howle,[4] Neil T. Hunt[1]

1. *Department of Chemistry and York Biomedical Research Institute, University of York, Heslington, York, YO10 5DD, UK*
2. *Department of Physics, University of Strathclyde, SUPA, 107 Rottenrow East, Glasgow, G4 0NG, UK*
3. *STFC Central Laser Facility, Research Complex at Harwell, Rutherford Appleton Laboratory, Harwell Campus, Didcot, OX11 0QX, UK*
4. *Defence Science and Technology Laboratory, Porton Down, Salisbury, SP4 0JQ, UK*

Abstract

Ultrafast 2D-IR spectroscopy is a powerful tool for understanding the spectroscopy and dynamics of biological molecules in the solution phase. A number of recent studies have begun to explore the utility of the information-rich 2D-IR spectra for analytical applications. Here, we report the application of ultrafast 2D-IR spectroscopy for the detection and classification of bacterial spores.

2D-IR spectra of *Bacillus atrophaeus* and *Bacillus thuringiensis* spores as dry films on CaF_2 windows were obtained. The sporulated nature of the bacteria was confirmed using 2D-IR diagonal and off-diagonal peaks arising from the calcium dipicolinate $CaDP{\cdot}3H_2O$ biomarker for sporulation. Distinctive peaks, in the protein amide I region of the spectrum were used to differentiate the two types of spore. The identified marker modes demonstrate the potential for the use of 2D-IR methods as a direct means of spore classification. We discuss these new results in perspective with the current state of analytical 2D-IR measurements, showing that the potential exists to apply 2D-IR spectroscopy to detect the spores on surfaces and in suspensions as well as in dry films. The results demonstrate how applying 2D-IR screening methodologies to spores would enable the creation of a library of spectra for classification purposes.

1. Introduction

Ultrafast 2D-IR spectroscopy has been applied to a broad range of systems, addressing questions relating to the role of ultrafast molecular dynamics in the behaviour of biological molecules, solutions and materials.[1-10] The 2D-IR spectrum provides a correlation map of excitation (pump) and detection (probe) frequency that contains features arising from coupling and energy transfer between vibrational modes. This means that a spectrum provides a unique 2D signature of a molecule that derives directly from its structure, bonding and local chemical environment. The macroscopic 3D nature of protein secondary structure provides an excellent example of the structure-linked 2D map, where amide I band coupling patterns are sensitive reporters of molecular structure and structural change.[11-14] An extra level of information arises from the availability of sub-ps dynamics through 2D-IR measurements, which

This is a peer-reviewed, accepted author manuscript of the following paper: Procacci, B., Rutherford, S. H., Greetham, G. M., Towrie, M., Parker, A. W., Robinson, C. V., Howle, C. R., & Hunt, N. T. (2021). Sensing of bacterial spores with 2D-IR spectroscopy. In J. A. Guicheteau, & C. R. Howle (Eds.), Chemical, Biological, Radiological, Nuclear, and Explosives (CBRNE) Sensing XXII [117490C] (Proceedings of SPIE - The International Society for Optical Engineering; Vol. 11749). SPIE. https://doi.org/10.1117/12.2585894

present both a means to follow dynamic behaviour in solution and to use vibrational energy flow as an additional source of diagnostic information.[15]

This ability to use 2D-IR spectroscopy as an information-rich map has inspired the development of 2D-IR for use as an analytical tool, a direction that has been significantly aided by the use of high repetition-rate laser systems that enable fast data collection.[16] Examples include combination of high throughput 2D-IR screening and principal component analysis (PCA) to screen and differentiate >2000 2D-IR spectra of DNA-ligand complexes.[17] 2D-IR spectroscopy has been applied to follow the formation of amyloid fibrils associated with type 2 diabetes and determine a multistep pathway involving a series of intermediates identified largely as β-sheet structures.[18] Microfluidic technology has been successfully interfaced with 2D-IR spectroscopy to study the sensitivity of the anion cyanate to the surrounding solvent environment and to monitor the vibrational response of cyanate in mixed solvent environments in a high-throughput manner.[19] Applications of 2D-IR for biomedically-relevant measurements have been reported, for example in the study of eye lens tissue from porcine and human subjects with and without cataracts.[20,21] An approach to measuring the amide I 2D-IR spectroscopy of proteins in H_2O based solvents has been reported, enabling measurements of proteins under physiological conditions, exploiting the link between protein secondary structure and the 2D-IR amide I lineshape for blood serum analysis.[22,23]

Bacillus anthracis is the causative agent of anthrax, and stand-off detection in the environment could have utility in both military and civilian contexts. In this article, we report the first attempt to use 2D-IR to study bacterial spores, focussing on the spore forming *Bacillus* genus. IR absorption spectroscopy has been applied successfully to the *Bacillus* genus, allowing discrimination to species level *via* spectral fingerprints that are unique for each microorganism. Furthermore, spectral libraries exist to relate absorbance to key functional groups,[24] while microbiological classification has been described in detail.[25,26] Recently, IR spectroscopy has been coupled to statistical data treatments to get faster and more accurate results. Diffuse reflectance infrared Fourier Transform spectroscopy (DRIFTS), for instance, has been used to discriminate between 36 strains of vegetative *Bacillus* cells and their spores.[27] Differences between different *Bacillus* species have been widely investigated *via* IR spectroscopy focusing on how to discern between the vegetative and sporulated forms.[28,29,30] The classification of spores of different soil bacilli and detection of bacterial spores in the presence of a clay mineral matrix has been achieved using attenuated total reflectance infra-red (ATR-IR) spectroscopy.[31] Very recently, an artificial neural network (ANN) assisted Fourier Transform Infra-Red (FT-IR) spectroscopy method was reported for the rapid and cost-efficient differentiation of closely related *Bacillus cereus* group members in different soils and food samples.[32]

Although a powerful tool, FT-IR spectroscopy cannot interrogate the amide I band to extract detailed information on the mixtures of proteins present in bacteria and spores, particularly in the protective coats of the latter, 2D- IR may therefore offer new ways to differentiate and classify species, while the off-diagonal region of the spectrum gives scope for disentangling complex spectral responses from these multi-component systems. Thus, our hypothesis is that 2D-IR will be able to provide an alternative route to classification and identification of samples as well as the ability to work in ‘wet’ environments as indicated by recent studies in blood serum.[22] Encouraged by the potential of analytical application of

2D-IR spectroscopy we tested a proposed protocol towards the detection and differentiation of two types of sporulated *Bacillus* bacteria.

2. Experimental

2.1. Preparation of bacterial spores

Bacillus atrophaeus NCTC 10073 (BG) and *Bacillus thuringiensis HD-1 Cry⁻ (Btcry⁻)*[33] were obtained from Defence Science and Technology Laboratory (Dstl) stocks. Spores were produced by inoculation of Leighton Doi[34] broth and incubation at 37°C with shaking at 180 rpm for 7 days. After incubation the spores were centrifuged at 8,000 rpm for 10 minutes and the supernatant discarded. The spore pellet was washed by resuspending in an equal volume of sterile distilled water and re-pelleting three more times before finally being resuspended in sterile distilled water to 10^9 cfu/ml (BG) or = 2.5 x 10^8 cfu/ml (*Btcry⁻*), as determined by plate counts on Tryptone Soya Agar. Spore preparations were confirmed by phase contrast microscopy to contain > 99 % spores with minimal observable cell debris.

2.2. Infrared spectroscopy

Sample preparation

A 15 μl volume of spore suspension was deposited on CaF_2 windows and allowed to dry (*BG* = 10^9 cfu/ml and *Btcry⁻* = 2.5 x 10^8 cfu/ml) at room temperature. An image of the dry films obtained *via* an optical microscope (Figure 1) showed that the films were inhomogeneous in terms of spore distribution. The white spot on the scale bars of the images represents the diameter of the overlap region of the laser beams used to collect the data (*ca* 150-200 μm) relative to the full sample; showing the area probed in each measurement. For experiments studying spores on a plastic surface, an aliquot of the spore suspension was deposited onto an IR-transmissive polypropylene surface and allowed to dry. The surface was then mounted into a standard cell holder for 2D-IR spectroscopy measurements.

IR absorption spectroscopy

All FT-IR spectroscopy measurements were performed on dry spore films using transmission geometry. Data were obtained using a Thermo Scientific Nicolet iS10 Fourier Transform spectrometer. Spectra were the result of 20 co-added scans at a resolution of 2 cm^{-1} in the spectral region 400–4000 cm^{-1}.

2D-IR spectroscopy

All 2D-IR data was collected using the Ultra B instrument at the STFC Rutherford Appleton laboratories.[35] Mid-IR pulses (bandwidth 400 cm^{-1}; pulse duration 50 fs; repetition rate 10 kHz) were produced *via* difference frequency generation of the signal and idler outputs of an optical parametric amplifier (OPA), which was in turn pumped by a regeneratively amplified Ti:sapphire laser system. All 2D-IR experiments were acquired using the Fourier transform method in which the two pump pulses and the probe pulse were arranged in a pseudo pump-probe geometry,[36,22] overlapping in, and passing through, the dry spore film. The pump frequency axis of the 2D-IR spectrum was obtained by Fourier

transformation of the time-domain signal with respect to the time delay between the two pump pulses, τ, which was controlled using a mid-IR pulse shaper.[37] The probe frequency axis was obtained by dispersion of the signal in a spectrograph and detection *via* liquid-nitrogen cooled 128-element MCT (mercury-cadmium-telluride) detectors, providing a spectral resolution of <2 cm^{-1}. In all experiments, perpendicular polarisation was employed alongside four-frame phase cycling of the pump pulse pair to limit contributions from pump light scattered by the sample. For each spectrum, data was obtained at 202 values of τ in steps of 15 fs to a final delay of 3 ps.

The 2D-IR experiments were carried out with the pump bandwidth centred at either 1650 cm^{-1} (protein amide I) or 1440 cm^{-1}, which was resonant with modes of the calcium dipicolinate ($CaDP{\cdot}3H_2O$) spore biomarker. In each case, two different regions of the spectrum were probed enabling one colour 2D-IR (same pump and probe wavenumber) and two colour 2D-IR (different pump and probe) experiments. The specific wavenumbers used are described in detail below. A total of five different waiting times (T_w, equivalent to the pump-probe delay time) were measured in each 2D-IR experiment (See SI). Each delay time was acquired using 600 seconds of averaging (6 M laser shots) or 900 s when pumping at 1440 cm^{-1}.

3. Results and discussion

Repeatability, scattering, polarization

Due to the inhomogeneous and scattering nature of the dry film samples, preliminary 2D-IR measurements were taken to determine the optimal measurement conditions. Scanning the measurement position across the sample showed that the intensity of the signal and the signal to noise ratio (SNR) varied depending on the position. Nevertheless, by sampling in different parts of the dry film the overall reproducibility of the spectra was found to be very good (See SI, Figure S2). All the experiments were conducted using perpendicular polarisation, which minimised scattering while maintaining a good signal intensity. This polarisation geometry is also the optimum for enhancing off-diagonal peaks in the 2D-IR spectrum relative to diagonal ones,[36,38] allowing access to both diagonal and off-diagonal regions of the 2D-IR spectrum and enhancing the chances of identifying peaks specific to the spore types studied.

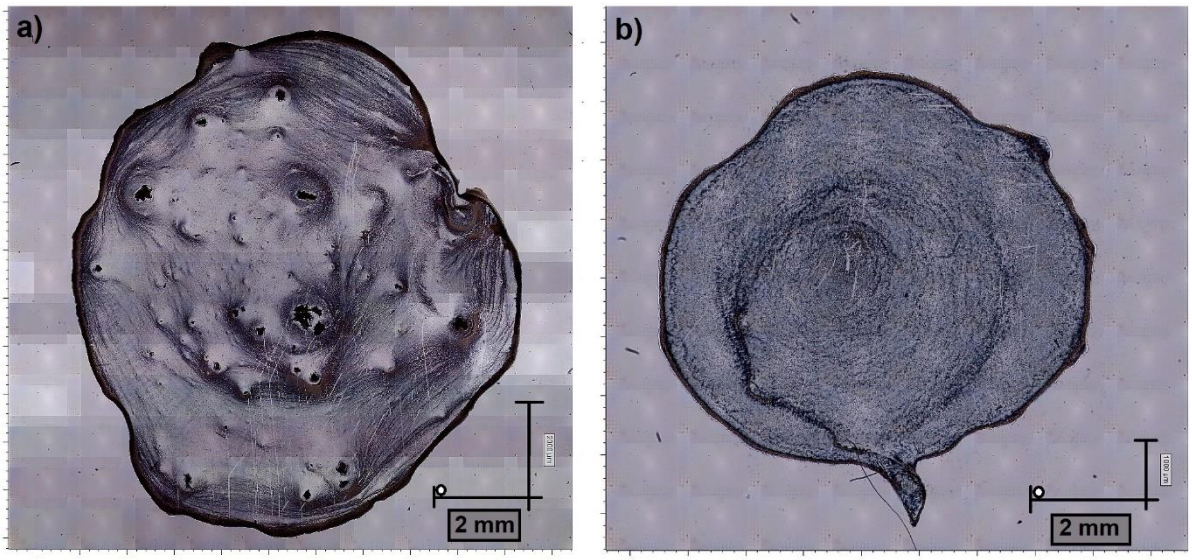

Figure 1. *Image of the dry films of bacterial spores of (a) BG and (b) Btcry- samples on a CaF_2 window. The image was obtained using a visible light microscope. Scale bars indicate the dimensions of the image. White spots on the scale bars indicate the size of the area interrogated by the laser beam (150-200 μm diameter) used to acquire the 2D-IR data.*

IR absorption

IR absorption spectra of dry films of *BG* and *Btcry-* (Figure 2(a)) contained the spectral features expected for endospores of a *Bacillus* species. Little difference was noted between the spectra of the two species, as confirmed by difference spectra (grey traces in Figure 2). The bands appear in four main regions of the spectrum: **W1** (3000 – 2800 cm^{-1}, See SI, Figure S1), which are assigned to stretching modes of unsaturated C-H moieties within fatty acids. **W2** (1800 – 1500 cm^{-1}, Figure 2) is dominated by amide I and amide II bands of proteins. **W3** (1500 -1200 cm^{-1}, Figure 2), contains bands from fatty-acids, proteins and phosphate groups and **W4** (1200 – 900 cm^{-1}, Figure 2) features bands mainly attributed to polysaccharides.[28]

For comparison, IR spectra were also recorded using ATR geometry (Figure 2(b)). In addition to the main vibrational spectroscopic features (**W1-4**), a new "quartet" of peaks (766, 725, 701 and 659 cm^{-1}) denoted **W5**, become visible. These bands, which were obscured by absorptions of the CaF_2 windows in transmission measurements, are typical of endospore samples and are assigned to bands originating from vibrations of calcium dipicolinate trihydrate ($CaDP{\cdot}3H_2O$, Figure 2).[29] The presence of $CaDP{\cdot}3H_2O$ in the spectra of spores provides a molecular signature with which to identify spores from vegetative cells. In addition to the low frequency quartet of peaks (**W5**) a further band at 1441 cm^{-1} (indicated by the arrow in the spectrum in Figure 2(a)) has also been assigned to pyridine ring vibration (ring CN stretch) of $CaDP{\cdot}3H_2O$.[29]

Based on these results, two regions of interest were identified for 2D-IR analysis of bacterial spores. **W2**, containing peaks arising from the amide I and II vibrational modes of proteins and **W3** which features calcium dipicolinate $CaDP{\cdot}3H_2O$ modes.[28] The experiments were divided into two sets, the

first at 1440 cm^{-1} to examine the response from $CaDP{\cdot}3H_2O$ (**W3**) and in the second set, the pump frequency was centred at 1650 cm^{-1} to probe the amide I region (**W2**).

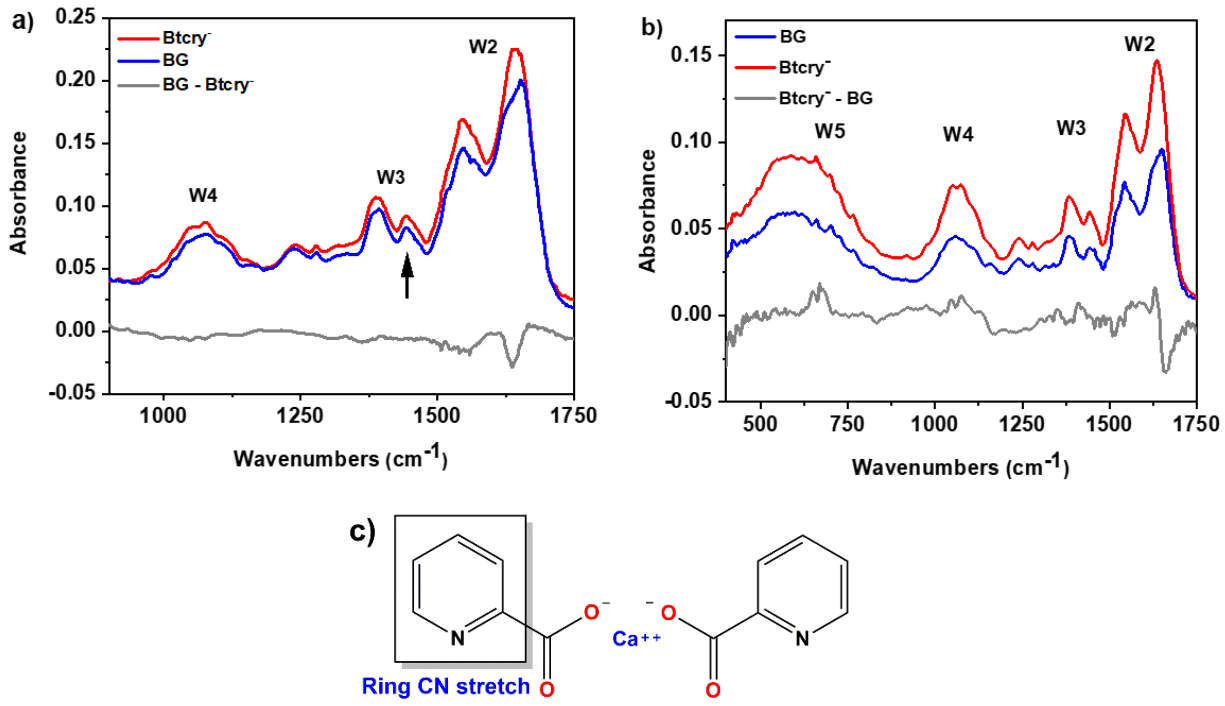

Figure 2. *a) FTIR spectra of a dry layer of the spores measured in transmission mode on CaF_2 windows, arrow highlights* 1441 cm^{-1} feature*, see text. b) ATR-IR spectra of a dry layer of spores (diamond prism). In both figures, the difference spectrum was obtained following normalization to the bands marked* ***W2****. c) $CaDP{\cdot}3H_2O$ structure. The functional group giving rise to bands in region* ***W3*** *is highlighted.*

3.1. 2D-IR spectroscopy

Excitation at 1440 cm^{-1} (W3): detection and identification of spores via the biomarker

This set of experiments was chosen to determine the two-dimensional response from excitation of the $CaDP{\cdot}3H_2O$ biomarker modes. Table 1 lists the relevant mode assignments.[30] The one colour 2D-IR spectra of *BG* and *Btcry⁻* spores (Figure 3) in this region show three peaks on the diagonal of the spectrum (red), located at 1390, 1440 and 1550 cm^{-1}. The positions of the two lower frequency peaks agree well with previously measured modes of $CaDP{\cdot}3H_2O$,[30] while the 1550 cm^{-1} peak is assigned to the amide II mode of the protein content of the spore.

In addition, the 2D-IR spectra show off-diagonal peaks that link a peak at 1375 cm^{-1} to modes at 1440 (dashed guide lines, Figure 3(a)) and 1395 cm^{-1}, these peaks arise from the presence of the biomarker $CaDP{\cdot}3H_2O$. Additional off-diagonal peaks are also observed linking modes near 1550 cm^{-1} to the $CaDP{\cdot}3H_2O$ modes at 1400 cm^{-1} and at 1440 cm^{-1} (solid guidelines in Figure 3(a)). This set of peaks is tentatively assigned to bands arising from different modes of the pyridine ring. It is worth noting that these extra bands are quite low in intensity due to the reduction in excitation energy available relative to the energy at 1650 cm^{-1} at this wavenumber, therefore their interpretation should be considered

tentative. Nevertheless, the frequencies are consistent with modes assigned to CaDP·3H_2O (Table 1) and are reproducible across different sets of data. The 2D-IR patterns are therefore identifiable as being attributable to the presence of the sporulated state of the bacteria. We note that neither the set of off-diagonal peaks to the 1550 cm^{-1} band (solid line, Figure 3(a)) nor the lower frequency band at 1375 cm^{-1} were detected for the *Btcry*$^-$ spore (Figure 3(b)) possibly due to the concentration of *Btcry*$^-$ being an order of magnitude smaller than *BG*.

Table 1. Measured and predicted prominent IR bands for CaDP·3H_2O along with spore frequencies[30]

CaDP 3H_2O in *Bacillus* Spore measured frequency (FT-IR)	**CaDP 3H_2O** measured frequency	**CaDP 3H_2O** SQM predicted frequency	**Approximate assignment** (% total energy distribution)
Between amides	1590 broad quartet		
	1632	1719	symmetric COO stretch, 59% CO
1585	1610	1708	asymmetric COO stretch, 59% CO
	1593	1625	45% HOH bend; 13% CaOH bend
1570	1570	1614	45% HOH bend; 19% CaOH bend
1467 shoulder	1466	1451	29% ring CC stretch; 26% in plane CCH bend
1441	1443	1420	34% ring CN stretch; 20% in plane CCH bend
1386 broad	1395	1323	29% CN str; 20% ring CC str; 10% C–O str
	1373	1315	symmetric COO str, 40% C-O; 20% C–C str
1277	1278	1245	asymmetric COO str, 40% C–O; 17% ring CC str

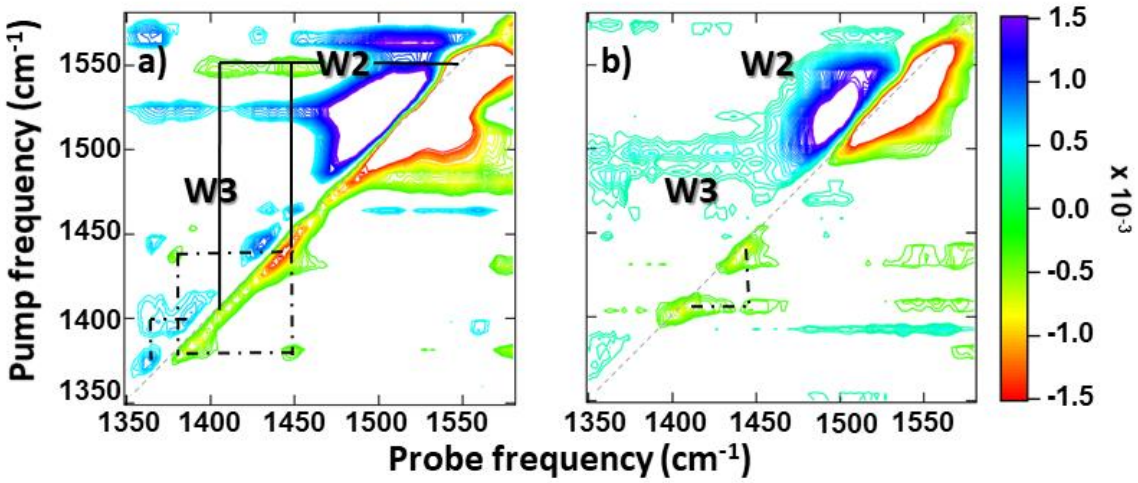

Figure 3. *2D-IR spectra measured with a waiting time (Tw) of 250 fs. a) BG and b) Btcry*$^-$ *showing the region* ***W2*** *for the amide II and* ***W3*** *for the biomarker CaDP·3H_2O; a filter (Savitzky – Golay, second order, 5 points) was applied and any countour below ± 0.003 was omitted for clarity.*

Excitation at 1650 cm^{-1} (W2): differentiation between the two spore types

Having established that peak patterns assignable to CaDP·3H$_2$O are visible in the 2D-IR spectra of the dry spore films, we progress to examine the amide I region of the spectrum (**W2,** Figure 4(a)) in order to investigate whether this spectral region provides a basis for species differentiation. The spore coat (*ca* 50% of the spore volume) is predominantly made up of proteins[30] and so the amide I mode is the strongest peak in the IR spectrum (Figure 2). The **W2** regions of the 2D-IR spectra of the *BG* and *Btcry*$^-$ spores (Figure 4(a) and (b)) are broadly similar. A pair of peaks near the diagonal at 1670 cm^{-1} (pump = probe frequency, dashed line) arises from the amide I band, which consists primarily of the CO stretching mode of the peptide linkage. The negative peak (red) centred at probe frequency of 1670 cm^{-1} is assigned to the v = 0-1 transitions of modes observed in the IR absorption spectrum whereas the positive peak (blue) is due to the v =1-2 transitions and so is observed at lower probe frequencies, shifted by vibrational anharmonicity. CaDP·3H$_2$O modes also contribute to this region of the spectrum, for example at 1632 cm^{-1} (Table 1), however the strong overlap of this band with the amide I renders these diagonal peaks hard to distinguish.

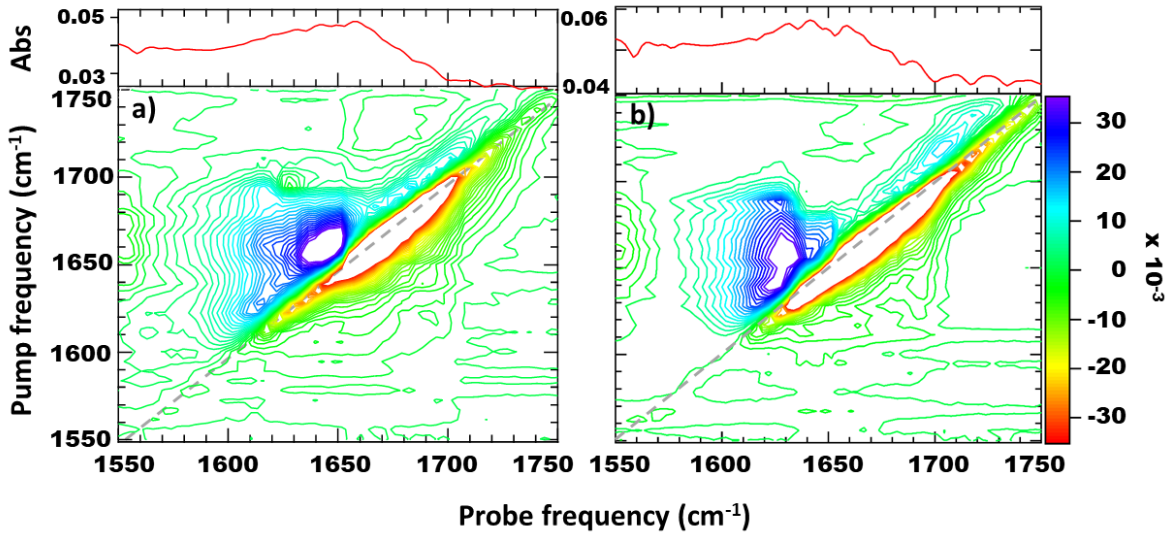

Figure 4. *2D-IR spectra of (a) BG and (b) Btcry*$^-$ *dry films measured with a waiting time (T_w) of 250 fs in the amide I region (**W2**). Corresponding FT-IR spectra are reproduced above.*

While the similarity of the spectra is to be expected based on the comparable chemical compositions of the two structures, subtle differences in the spectra of the two species were resolvable. In particular, the shape of the v=1→2 portion of the *Btcry*$^-$ spectrum (Figure 4(b)) indicates possible variations in off-diagonal structure or anharmonicity of the amide I band relative to *BG* (Figure 4(a)). It has been shown previously that the anharmonicity of the amide I band reduces in larger, less dynamic secondary structural units due to increased vibrational coupling. ~~The~~ This implies that the anharmonicity ~~latter~~ is linked to integrity of secondary structure units within a protein., ~~becoming reduced as vibrational~~

~~coupling increases~~.[39] Although it is hard to be definitive in a complex matrix such as a spore, this observation indicates chemical variations between the two species of spores and spectroscopic signatures that are usable as a means of differentiation.

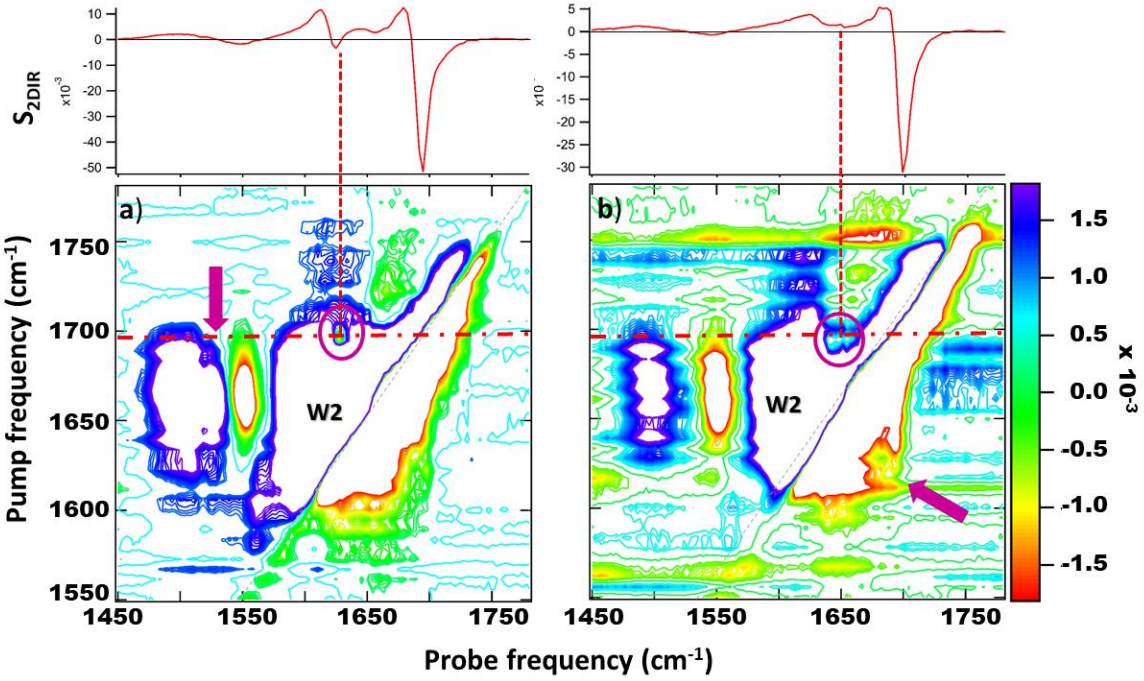

Figure 5. *2D-IR spectra of (a) BG (a) and (b) Btcry- measured with a waiting time (T_w) of 250 fs. The circles and arrows underline the different peaks discussed in the text. Any countour between ± 0.003 was omitted for clarity. Cross sections through the spectra at a pump frequency of 1690 cm-1 (horizontal dashed-dotted red line) are reproduced above the spectra (see text).*

Closer inspection reveals further differences between the 2D-IR spectra of *BG* and *Btcry-* that were reproducible across the series of measurements performed (Figure 5). Specifically, the *BG* spectrum (Figure 5(a)) displays a cross peak at (pump, probe) = (1695, 1625 cm^{-1}) (purple circle), which appears superimposed upon the v=1-2 portion of the amide I response. Such a feature is absent in the *Btcry-* spectrum, though a feature is observed at (1690, 1650 cm^{-1}), which hints at a cross peak or is possibly a function manifestation of the different v=1-2 peakshape noted in reference to Figure 4.

Overall, the 2D-IR spectral features identified above whilst spectrally across a narrow window do not coincide with peaks previously assigned to CaDP, suggesting that they are related to the amide I band of the spore. It is noteworthy that the peak positions indicated (1620 and >1680 cm^{-1}) for the peak in the *BG* spectrum are consistent with those associated with a large, well-ordered β-sheet type structures, an observation that is consistent with the generally smaller v=0-1 to v=1-2 anharmonic separation observed for *BG* spores. Other evidence of differences between *BG* and *Btcry-* are observed in the *BG* spectrum at (1660, 1525 cm^{-1}), shown by a purple arrow in Figure 5(a), which indicate differences in the shape of the amide I – amide II off-diagonal feature.[39]

Taken together, all these deviations between spectra of *BG* and *Btcry-* can be considered as representing a different protein secondary structure content that is resolved by the off-diagonal information of the 2D-IR spectra, and we further emphasize this point through illustrating a cross section

of the 2D-IR data (Figure 5). As always, directly linking vibrational spectral signatures to chemical structure and quantitative analysis in complex biological molecules remains challenging. Whilst here we can only presently speculate on the information hidden within the data, the differences are real and show a species specific dependence. The presence of these differences in the off-diagonal region of the spectrum means that they would not necessarily be detected by IR absorption methods.[40] Another contributory factor is the manifestation of secondary structure couplings *via* increased amplitudes of 2D-IR signals,[22,39,41] whereby 2D-IR spectroscopy tends to amplify signals from macromolecular structures, enhancing its ability to identify small changes over IR absoprtion methods.

Examining the off-diagonal region of the 2D-IR spectrum when exciting the amide I band shows that the spectra of both *BG* and *Btcry*$^-$ display expected major cross peaks between the amide I - II bands at (1650, 1550 cm^{-1}) as well as additional off-diagonal peaks apparently linking diagonal features near 1610 cm^{-1} to bands near probe frequencies of 1400 and 1440 cm^{-1} (Figure 6, dashed guide lines). These agree well with bands of the biomarker calcium dipicolinate (Table 1) and may arise from excitation of higher frequency bands from CaDP·3H_2O which overlap with the amide I mode. This is reinforced by the fact that the centre of mass of the off-diagonal peaks appears to be at pump frequencies between 1600 and 1650 cm^{-1}, whereas the amide I band is biased towards frequencies greater than 1650 cm^{-1}. Protein bands possibly linked to deprotonated carboxylic moieties might also appear in this region. It should be noted that the signal strength is weak and these assignments are therefore tentative.

This data suggests a means to determine the presence of the spore form of the bacterium and a means to identify the type in a single spectrum. This is possible because a 2D-IR spectrum with a pump frequency centred on 1650 cm^{-1} and probing the range from 1700-1350 cm^{-1} can resolve not only the amide I band, where differences in bacterial species appear but also off-diagonal peaks which reveal to presence of peaks due to the sporulation biomarker.

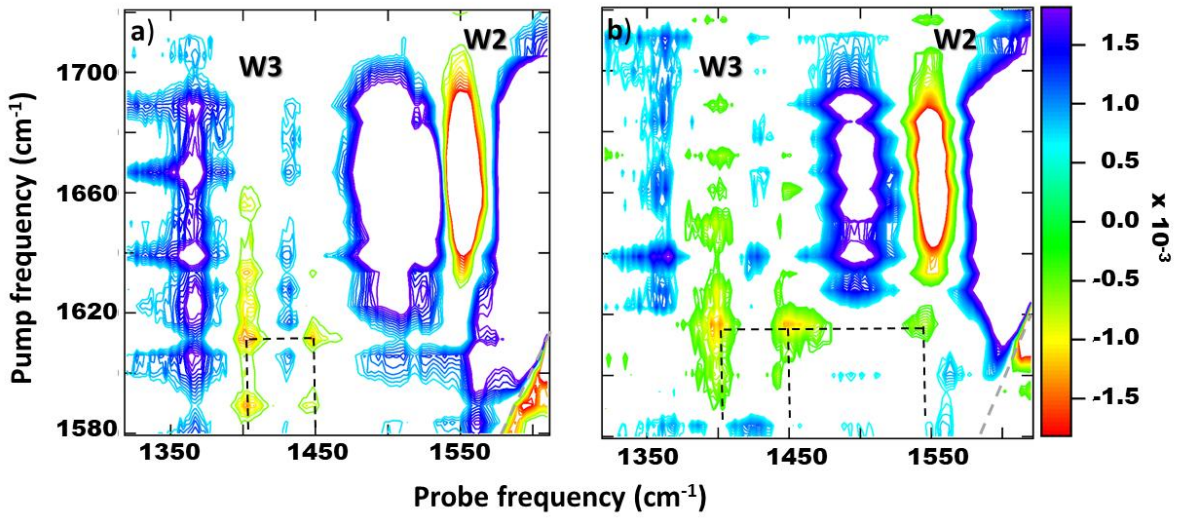

Figure 6. *2D-IR spectra of BG (a) and Btcry$^-$ (b) measured with a waiting time (Tw) of 250 fs. Any countour below ± 0.005 was omitted for clarity.*

BG and Btcry⁻ on a plastic surface (polypropylene), pumping at 1650 cm^{-1}

In order to demonstrate the applicability of the 2D-IR technique to real world surfaces (e. g.other than CaF_2), the spores were also probed on an IR transmissive plastic surface. Although the quality of signals obtained was lessened by high light scattering, sufficient quality was achieveable to permit a comparable level of analysis to that performed for the CaF_2 substrates (Figure 7). The amide I mode is the predominant peak on the spectrum diagonal, however the distinctive peaks for the *BG* spores previously identified (purple circles on the spectra in Figure 7) are detectable and the differences in general amide I lineshape are resolvable. This result is encouraging as it indicates the potential of detecting and differentiating the spores on different surfaces. Probing and pumping the **W3** region of the spectrum was impossible due to strong absorption by polypropylene modes that overlap with the biomarker CaDP·3H_2O bands.

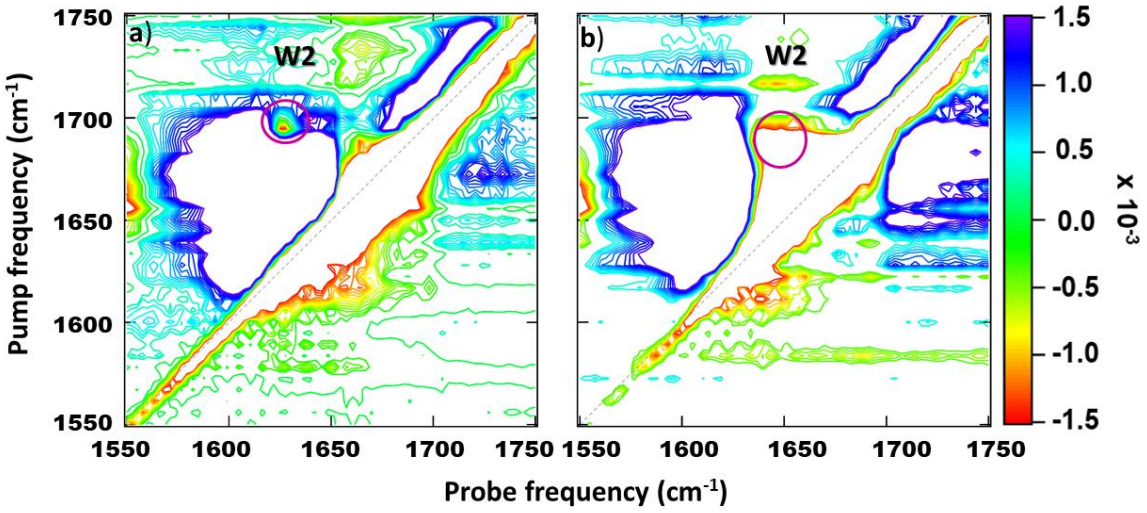

Figure 7. *2D-IR spectra of a (a) BG and (b) Btcry⁻ dry film on a polypropylene surface in the amide region* ***W2****. The spectra were measured with a waiting time (T_w) of 250 fs. The purple circles highlight the differences between the two spores. Any countour below ± 0.005 was omitted for clarity.*

4. Conclusions

2D-IR spectroscopy has proved to be a successful approach to detecting and differentiating *Bacillus* spores from two different species in a robust and reproducible way. Furthermore, in the same measurement, 2D-IR is able to infer the presence of the spore form of the bacteria *via* modes of the known marker chemical CaDP·3H_2O. The set of data collected led to spore detection on CaF_2 windows and on a plastic surface. The identified marker modes yielded a number of peaks that varied between the two species of *Bacillus* spore studied, giving potential routes for use in spore classification. In particular, distinctive peaks were singled out for the *BG* and *Btcry⁻* that identify chemical or structurally specific differences and we tentatively ascribe our findings as consistent with changes in the β-sheet

morphology of one or more proteins. Clearly further work is necessary on a broader range of *Bacillus* spores to support and extend these findings.

We have previously demonstrated that PCA coupled to 2D-IR spectroscopy can be used for rapid screening and discrimination of DNA-ligand complexes.[17] The same approach could be applied to spore discrimination. The potential for using 2D-IR spectroscopy for measuring proteins in water, also recently demonstrated,[22] becomes relevant to measuring the spores in suspensions rather than as dry films and opens up the possibility of studying the vegetative form of *Bacillus* bacteria. Screening a wide range of bacteria under different conditions (e.g. spores/vegetative; dry film/suspension) with 2D-IR spectroscopy would allow the build-up of a library of spectra from which variances can be determined by computational analysis (e.g. machine learning). These differences would exploit the additional information content of 2D-IR in comparison to FTIR methods and so could be used to build a more general and accessible way to facilitate the detection and differentiation between *Bacillus* species of the same form (vegetative or sporulated) and across the two forms. A wider study across different *Bacillus* spores and the spectroscopic understanding of the vegetative form of the bacteria using 2D-IR spectroscopy would further complement our findings. Finally, the possibility of using reflection detection geometry (*e.g*. ATR) could also expand the applicability of the technique allowing probing the bacteria on different surfaces.[42]

Declaration of Competing Interest

The authors declare that they have no known competing financial interests or personal relationships that could have appeared to influence the work reported in this paper.

Acknowledgment

We are grateful to the UK Ministry of Defence for funding via the Defence and Security Accelerator (DSTLX1000131398) and Dr. Daniel Shaw for useful discussions. We acknowledge STFC for facility access to the ULTRA laser system and Dr. Emma Gozzard for technical assistance.

5. References

[1] R. M. Hochstrasser, *Proc. Natl. Acad. Sci*., **2007**, 104, 14190. doi.org/10.1073/pnas.0704079104

[2] Z. Ganim, H. S. Chung, A. W. Smith, L. P. Deflores, K. C. Jones and A. Tokmakoff, *Acc. Chem. Res*., **2008**, 41, 432. doi.org/10.1021/ar700188n

[3] J. Bredenbeck, J. Helbing, C. Kolano and P. Hamm, *ChemPhysChem*, **2007**, 8, 1747. doi.org/10.1002/cphc.200700148

[4] A. Ghosh, J. S. Ostrander, M. T. Zanni, *Chem. Rev*., **2017**, 117, 10726. doi.org/10.1021/acs.chemrev.6b00582

[5] G. Hithell, L. A. I. Ramakers, G. A. Burley and N. T. Hunt, in Frontiers in Molecular Spectroscopy, ed. J. Laane, Elsevier, **2018**, 77.

[6] N. T. Hunt, *Dalton Trans*., **2014**, 43, 17578. doi.org/10.1039/C4DT01410C

[7] K. Adamczyk, M. Candelaresi, K. Robb, A. Gumiero,M. A. Walsh, A. W. Parker, P. A. Hoskisson, N. P. Tucker and N. T. Hunt, *Meas. Sci. Technol*., **2012**, 23, 062001. doi.org/10.1088/0957-0233/23/6/062001

[8] N. T. Hunt, *Chem. Soc. Rev*., **2009**, 38, 1837. DOI: 10.1039/B819181F

[9] A. L. Le Sueur, R. E. Horness. M. C. Thielges, Analyst, **2015**, **140**, 4336. DOI: 10.1039/c5an00558b

[10] L. M. Kiefer, K. J. Kubarych, *Coord. Chem. Rev.,* **2018**, 372, 153. doi.org/10.1016/j.ccr.2018.05.006

[11] C. R. Baiz, C. S. Peng, M. E. Reppert, K. C. Jones, A. Tokmakoff, *Analyst*, **2012**, 137, 1793. DOI: 10.1039/C2AN16031E

[12] I. J. Finkelstein, H Ishikawa, S. Kim, A. M. Massari, M. D. Fayer, *Proc. Natl. Acad. Sci*, **2007**, 104 (8), 2637. doi.org/10.1073/pnas.0610027104

[13] N. Demirdöven, C. M. Cheatum, H. S. Chung, M. Khalil, J. Knoester, A. Tokmakoff, *J. Am. Chem. Soc*., **2004**, 126, 25, 7981. doi.org/10.1021/ja049811j

[14] D. J. Shaw, R. E. Hill, N. Simpson, F. S. Husseini, K. Robb, G. M. Greetham, M. Towrie, A. W. Parker, D. Robinson, J. D. Hirst, P. A. Hoskisson, N. T. Hunt, *Chem. Sci.*, **2017**,8, 8384. DOI: 10.1039/C7SC03336B

[15] N. I. Rubtsova, I. V. Rubtsov, *Annu. Rev. Phys. Chem*., **2015**, 66, 717. doi.org/10.1146/annurev-physchem-040214-121337

[16] R., Fritzsch, S., Hume, L., Minnes, M. J., Baker, G. A., Burley and N. T., Hunt, *Analyst*, **2020**, 145, 2014. DOI: 10.1039/C9AN02035G

[17] R., Fritzsch, P. M., Donaldson, G. M., Greetham, M., Towrie, A. W., Parker, M. J., Baker and N. T., Hunt, *Anal. Chem.,* **2018**, 90, 2732. doi.org/10.1021/acs.analchem.7b04727

[18] S-H Shima, R. Guptab, Y. L. Linga, D. B. Strasfelda, D. P. Raleighb, M. T. Zanni, *Proc. Natl. Acad. Sci.,* **2009,** 106, 16,6614. doi.org/10.1073/pnas.0805957106

[19] K. M. Tracy, M. V. Barich, C. L. Carver, B. M. Luther, A. T. Krummel, *J. Phys. Chem. Lett.,* **2016**, 7, 4865. doi.org/10.1021/acs.jpclett.6b01941

[20] A. M. Alperstein, J. S. Ostrander, T. Q. O. Zhang and M. T. Zanni, *Proc. Natl. Acad. Sci.*, **2019**, 116, 6602. doi.org/10.1073/pnas.1821534116

[21] T. O. Zhang, A. M. Alperstein and M. T. Zanni, *J. Mol. Biol*., **2017**, 429, 1705. doi.org/10.1016/j.jmb.2017.04.014

[22] S. Hume, G. Hithell, G. M. Greetham, P. M. Donaldson, M. Towrie, A. W. Parker, M. J. Baker and N. T. Hunt, *Chem. Sci*., **2019**, 10, 6448. DOI: 10.1039/C9SC01590F

[23] S. Hume, G. M. Greetham, P. M. Donaldson, M. Towrie, A. W. Parker, M. J. Baker, N. T. Hunt, *Anal. Chem.,* **2020**, 92, 3463. doi.org/10.1021/acs.analchem.9b05601

[24] Yu, C; Irudayaraj, J; *Biopolymers*, **2005**, 77, 368. doi.org/10.1002/bip.20247

[25] Naumann, D; In Modern techniques for rapid microbiological analysis. Edited by Nelson WH. New York: VCH Publishers; **1990**, 43.

[26] Helm, D., Labischinski, H., Schallehn, G., Naumann, D., *J. Gen. Microbiol*., **1991**, 137, 69. doi.org/10.1099/00221287-137-1-69

[27] R., Goodacre, B., Shann, R. J., Gilbert, E. M., Timmins, A. C., McGovern, B. K., Alsberg, D. B., Kell, N. A., Logan., *Anal. Chem*., **2000**, 72, 1, 119. doi.org/10.1021/ac990661i

[28] N. S., Foster, S. E., Thompson, N. B. Valentine, J. E., Amonette, T. A., Johnson, *Appl. Spectrosc.*, 58, 2, **2004**, 203. doi.org/10.1366/000370204322842940

[29] J.B., Forrester, N. B., Valentine, Y. F., Su, T. J. Johnson, *Anal. Chim. Acta*, **2009**, 651, 24. doi.org/10.1016/j.aca.2009.08.005

[30] T. J., Johnson, S. D., Williams, N. B. Valentine, Y. F., Su, *Appl. Spectrosc.,* **2009**, 63, 8:908. PNNL-SA-64041

[31] A., Brandes Ammann, H. Brandl, *BMC Biophysics,* **2011**, 4, 14. doi.org/10.1186/2046-1682-4-14

[32] M. Bagcıo, M. Fricke, S. Johler, M. Ehling-Schulz, Frontiers in Microbiology, **2019**, 10, article 902. 10.3389/fmicb.2019.00902

[33] A.H. Bishop, C.V. Robinson, *J. Appl. Microbiol.,* **2014**, 117, 1274. doi.org/10.1111/jam.12620

[34] T. J. Leighton,R. H. Doi, *J. Biol. Chem*.,**1971,** 246(10), 3189.

[35] G. M., Greetham, P., Burgos, Q., Cao, I. P., Clark, P. S., Codd, R. C., Farrow, M. W., George, M., Kogimtzis, P., Matousek, A. W., Parker, M. R., Pollard, D. A., Robinson, Z.-J., Xin, M., Towrie, *Appl. Spectrosc*., **2010**, 64, 1311. www.osapublishing.org/as/abstract.cfm?URI=as-64-12-1311

[36] L. P. DeFlores, R. A. Nicodemus, A. Tokmakoff, *Opt. Lett*., **2007**, 32, 2966. doi.org/10.1364/OL.32.002966

[37] C. T. Middleton, D. B. Strasfeld, M. T. Zanni, *Opt. Express*., **2009**; 17(17): 14526. doi.org/10.1364/OE.17.014526

[38] M. T. Zanni, N-H Ge, Y., Kim, R. M. Hochstrasser, *Proc. Natl. Acad. Sci,* **2001**, 98, 20, 11265. doi.org/10.1073/pnas.201412998

[39] J. P. Lomont, J. S. Ostrander, J-J. Ho, M. K. Petti, M. T. Zanni, *J. Phys. Chem. B*, **2017**, 121, 38, 8935. doi.org/10.1021/acs.jpcb.7b06826

[40] L. P. DeFlores, Z. Ganim, R. A. Nicodemus, A Tokmakoff, *J. Am. Chem. Soc*., **2009**, 131, 3385. doi.org/10.1021/ja8094922

[41] L. Minnes, D. J. Shaw, B. P. Cossins, P. M. Donaldson, G. M. Greetham, M. Towrie, A. W. Parker, M. J. Baker, A. J. Henry, R. J. Taylor, N. T. Hunt, *Anal. Chem*., **2017**, 89, 10898. doi.org/10.1021/acs.analchem.7b02610

[42] J. P. Kraack, P. Hamm, *Chem Rev.,* **2017**, 117, 10623. doi.org/10.1021/acs.chemrev.6b00437